Available online at www.sciencedirect.com
ScienceDirect
Trans. Nonferrous Met. Soc. China 25(2015) 3928−3935
Transactions of Nonferrous Metals Society of China
www.tnmsc.cn

Enhanced ductility and reduced asymmetry of Mg−2Al−1Zn alloy plate processed by torsion and annealing

Jun WANG[1,2], Xu-yue YANG[1], Yi LI[1], Zhen-yu XIAO[1], Du-xiu ZHANG[1], Taku SAKAI[3]

1. Key Laboratory of Nonferrous Metal Materials Science and Engineering, School of Materials Science and Engineering, Central South University, Changsha 410083, China;
2. Institute for Frontier Materials, Deakin University, Geelong 3125, Australia;
3. The University of Electro-Communications, Tokyo 182-8585, Japan

Received 1 February 2015; accepted 20 September 2015

Abstract: The ductility and plastic asymmetry of an as-annealed magnesium alloy plate were studied in compression through combined process of torsion and subsequent annealing by optical microscope and EBSD. The yield strength (YS) and ultimate compression strength (UCS) as well as the compression ductility (CD) were simultaneously raised by prior torsion at room temperature. The CD was further enhanced by subsequent annealing. Also, the torqued sample followed by annealing experienced a rising CD with the increase in prior strain, leading to the maximum true strain of 0.279, which is twice that of the as-annealed original one. The sample showed a largely reduced tension−compression yield asymmetry by subjecting to pre-torsion alone or combined with a subsequent annealing. The enhanced ductility and reduced asymmetry are attributed to the development of a gradient microstructure with refined grains, and also randomization of the weakened texture due to torsion and subsequent annealing.
Key words: magnesium alloy; microstructure; torsion; asymmetry; texture; twinning

1 Introduction

Magnesium (Mg) alloys have attracted a growing attention from every sector of the metal consuming industries due to their low density and high specific strength, especially in the automotive industry where lightweight structural alloys are desired as a result of the increasing need for the improved fuel economy [1]. In order to satisfy the need of industry, wrought alloys are manufactured, usually in the form of rolling or extrusion. Rolled and extruded Mg alloys generally exhibit low ductility at room temperature because of the limited slip systems in hexagonal close-packed (HCP) structure and the resultant strong basal texture [2−5]. The presence of deformation texture of Mg alloys often results in intensive tension–compression yield asymmetry [6−8]. It is well known that grain refinement and texture modification are effective in enhancing the ductility and reducing the asymmetry of Mg alloys [7−11]. Many reports [12,13] suggest that the introduction of simple shear strain into Mg alloys can be a promising approach for the texture control. Torsion is an efficient way of providing simple shear strain for the samples. During tension or compression, the principal stresses/strains do not change their directions during deformation; however, under torsion, the direction of shear strain alters with deformation, thereby providing a possible way to change and optimize the microstructure and texture. However, quite a few studies on the torsion of Mg alloys have been reported and most of them were related to the Swift effect [14−16], or the microstructure and texture evolution brought up by torsion up to a very large strain at elevated temperatures [17]. To the best of our knowledge, the application of torsion has not been applied as a method to improve the mechanical properties of Mg alloys.

The present study was aimed to optimize the mechanical properties, especially the ductility and asymmetry of an as-annealed Mg alloy plate through a combined process of torsional deformation and subsequent annealing. The microstructures and texture

Foundation item: Project (51474241) supported by the National Natural Science Foundation of China; Project (2013CB632204) supported by the National Basic Research Program of China
Corresponding author: Xu-yue YANG; Tel: +86-731-88876470; E-mail: yangxuyue@csu.edu.cn
DOI: 10.1016/S1003-6326(15)64040-7

developed under such processes and the resultant mechanical properties were examined. The results were analyzed and the mechanisms operated were discussed.

2 Experimental

A commercial hot-rolled Mg alloy AZ21 (Mg−2.0Al−1.0Zn, mass fraction, %) plate with a thickness of 12 mm was annealed at 673 K for 2 h and used as the starting materials. The orientation imaging microscopy (OIM) microstructure and its corresponding (0001) and $(10\bar{1}0)$ pole figures of the initial material are presented in Fig. 1. The sample was composed of a twin-free equiaxed grains structure with an average linear intercept grain size of around 65 μm. The initial texture, measured by the electron backscatter diffraction (EBSD) technique, showed an intense basal texture with most basal planes aligned parallel to the rolling plane and also with a randomly oriented *a*-axis along the rolling plane. Cylindrical torsion specimens were prepared with their axial directions along the transverse direction of the Mg plate. The gauge section was 80 mm in length and 8 mm in diameter. The samples were twisted in one direction with one side rotary torsion testing machine at a rotation speed of 1 r/min and room temperature. The shear strain was calculated by [14]

$$\gamma=r\theta/L \quad (1)$$

where γ is the shear strain, r is the distance from the center, θ is the rotation angle, and L is the gauge length. Here, γ represents the maximum shear strain on the outer surface of the rod.

For compression tests of the torqued samples, specimens with 10 mm in height were machined along the axial direction. Some of them were subsequently annealed at 573 K for 1 h and water quenched. For tensile tests, on the other hand, a sample with a gauge length of 10 mm and a gauge diameter of 6 mm was wire-cut. The compression and tensile tests were carried out using Instron-type mechanical testing machine at an initial strain rate of $3\times10^{-3}s^{-1}$ and room temperature. The microstructures developed were examined by optical microscopy (OM) and OIM, and the textures were analyzed by EBSD in a field emission gun equipped with scanning electron microscope. The Vickers hardness tests were carried out in the following three zones of the cross-section of each cylindrical sample, i.e., the central region (r=0−0.5 mm), the middle one (r=1.7−2.3 mm) and the outer one (r=3−4 mm). The central and outer regions of the sample were also selected for the EBSD test. In order to compare the hardness changes in the specific zones, these hardness values were derived from almost the same part of the sample of two different states. For each specific zone, 7 measurements were obtained within 0.2 mm in terms of the distance from central point on the cross section of the sample. Finally, these 7 measurements were averaged and the results were used to draw the Vickers hardness distribution graph. The error bars were also provided.

3 Results

3.1 Mechanical properties

Compressive true stress−true strain curves are depicted in order of the prior-shear strain in Fig. 2 for AZ21 alloy in different states, i.e., as-annealed, prior-torqued and prior-torqued followed by annealing.

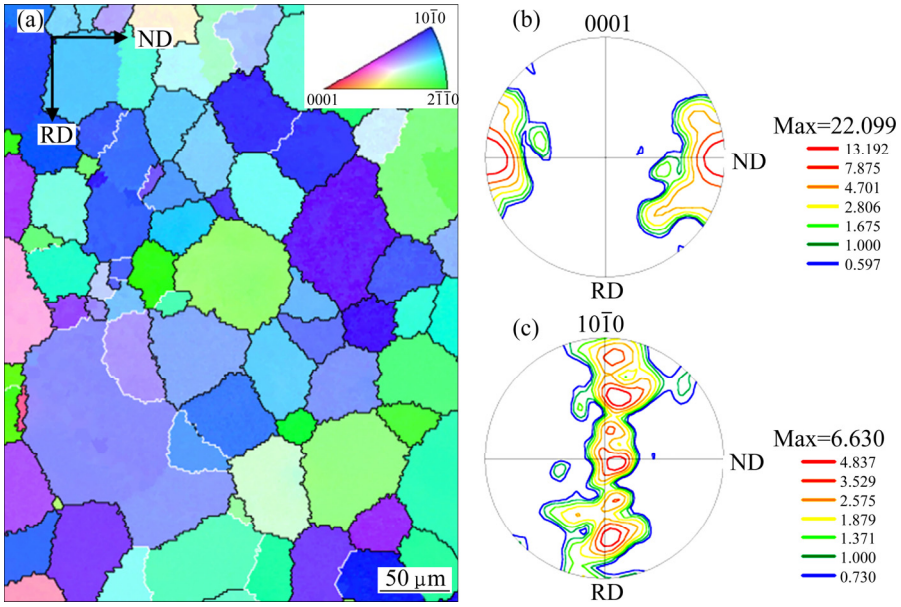

Fig. 1 Microstructural characteristics of as-annealed sample: (a) OIM image; (b) (0001) pole figure; (c) $(10\bar{1}0)$ pole figure

The mechanical properties derived from the flow curves in Fig. 2 are summarized in Table 1. True strains at facture were used to represent the compression ductility (CD) of sample. When the as-annealed sample was prior-torqued to three levels of shear strain, i.e., γ= 0.087, 0.175 and 0.262, the yield strength (YS), ultimate compression strength (UCS) and CD were all raised compared with those of the as-annealed one, although only slightly for UCS and CD. With subsequent annealing, the ductility is further greatly enhanced accompanying with a slight drop (less than 13 MPa) in UCS but a considerable decrease (40−60 MPa) in YS. It is remarkable to note that the sample torqued to γ=0.262 followed by annealing shows the highest ductility as much as 0.279, which is twice that of the as-annealed one (0.136).

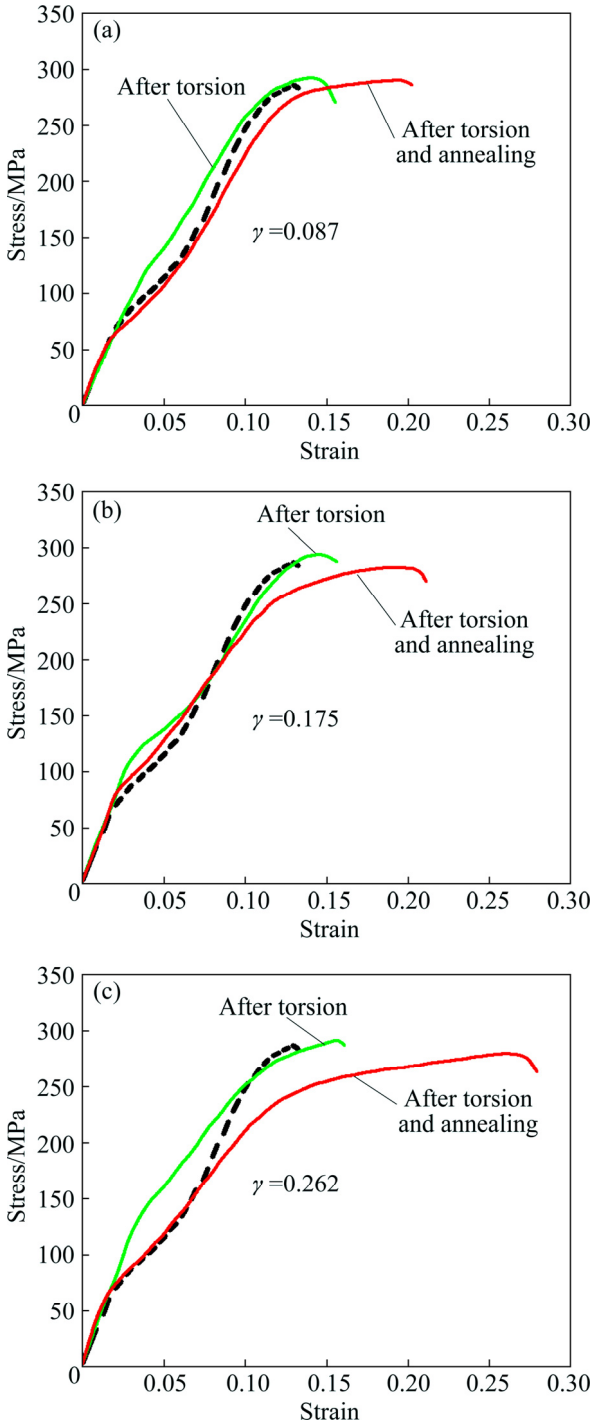

Fig. 2 True stress−true strain curves under compression at room temperature for samples torqued and subsequently annealed (The flow curve for the as-annealed sample is indicated by a broken line in each figure for comparison)

Table 1 Effect of prior-torsion and subsequent annealing on compression yield stress (CYS), ultimate compressive stress (UCS), and compressive ductility (CD) for as-rolled Mg alloy AZ21

Treatment	Applied shear strain, γ	CYS/MPa	UCS/MPa	CD
Prior-torsion	0	74	286	0.136
	0.087	126	293	0.152
	0.175	126	293	0.156
	0.262	135	291	0.161
Prior-torsion/ annealing	0.087	70	290	0.202
	0.175	86	280	0.211
	0.262	75	279	0.279

3.2 Reduction of asymmetry

At γ=0.262 followed by annealing, the sample showed the highest ductility, it would be interesting to study further its tension and compression asymmetry properties. Figure 3 shows the true stress−true strain curves of tension and compression tests of the Mg alloy samples at different states, namely, as-annealed, prior-torqued at γ=0.262 and prior-torqued followed by annealing. It is seen that compressive flow curves (black lines) have obviously different characteristics compared with those of the tensile tests (blue lines). In order to clarify and compare the yield strength measured by compression and tension, both the compressive and tensile yield strengths are summarized in Table 2. It is

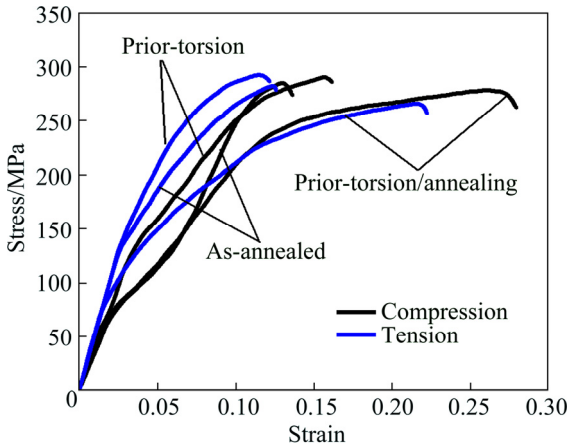

Fig. 3 True stress−true strain curves of tension and compression tests of samples under different conditions

Table 2 Mechanical properties of as-annealed, prior-torsion (γ=0.262), and prior-torsion/ annealing samples

Treatment	Test mode	YS/MPa	CYS/TYS
As-annealed	Compression	74	0.55
	Tension	135	
Prior-torsion	Compression	135	0.95
	Tension	142	
Prior-torsion/ annealing	Compression	75	0.83
	Tension	90	

TYS—Tension yield strength

seen that both prior-torsion and prior-torsion followed by annealing can reduce the tension−compression yield asymmetry, i.e., the ratio of compressive yield strength to tensile yield strength, to 0.95 and 0.83 from 0.55 of the as-annealed sample.

3.3 Microstructures and corresponding hardness

Figure 4 shows the microstructures evolved in the center and outer regions of the sample torqued to γ=0.262 as well as the ones followed by annealing. The hardness changes accompanied by these processes are plotted against distance from the center of the sample in Fig. 5. It is seen in Figs. 4(a) and (b) that many lenticular twins are frequently evolved and cross the original grains [18]. In the central region, recovered and coarse grains are evolved almost fully, and some lamellar twins are still remained (Fig. 4(c)). In contrast, much finer grains are fully developed in the outer region after annealing as presented in Fig. 4(d). Concurrently, the hardness decreases from HV 74.6 to HV 61.2 for the outer region and from HV 63 to HV 59 for the center one (Fig. 5).

3.4 Texture changes

In order to investigate the texture evolution and the deformation mechanisms involved in torsion and annealing, EBSD analysis was carried out on the samples torqued to γ=0.262 and subsequent annealing at 573 K for 1 h. Representative OIM maps, (0001) pole figures and grain boundary maps in the central and outer regions of the sample are presented in Fig. 6. In OIM maps, colors correspond to crystallographic orientation in the inverse pole figures. In the grain boundary maps, black lines correspond to boundaries of misorientation ≥3°, the red lines stand for the misorientation of (86±2)° and thick-blue lines for (56±2)°, which are proven to be the boundary of $\{10\bar{1}2\}$ extension twins and $\{10\bar{1}1\}$ compression twins, respectively [11]. It is seen that $\{10\bar{1}2\}$ extension twins are much more likely to be activated than $\{10\bar{1}1\}$ compression twins during

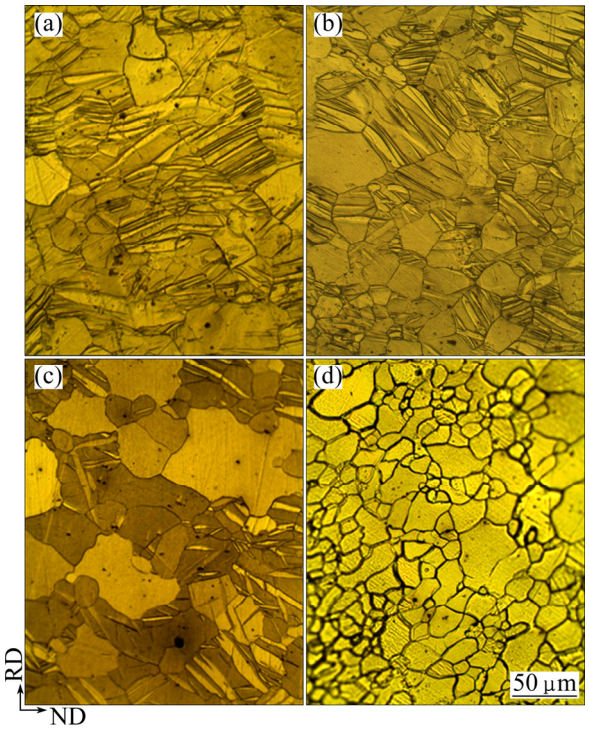

Fig. 4 Optical micrographs in central (a) and outer (b) regions of samples twisted to γ=0.262 and then followed by annealing (c) and (d), respectively

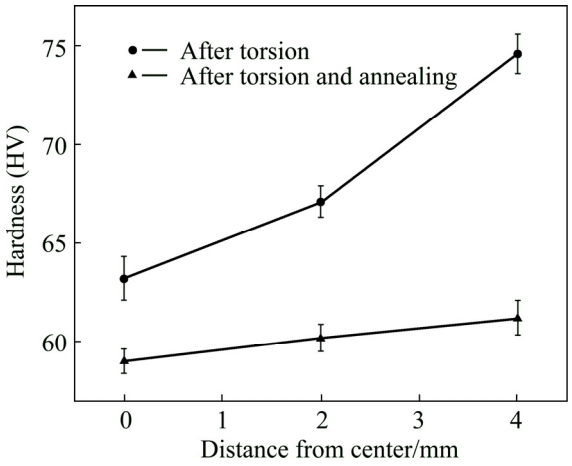

Fig. 5 Vickers hardness distribution along cross section of cylindrical samples twisted to γ=0.262 and then followed by annealing

torsion at room temperature. From the OIM maps, it is noted that the initial orientation is greatly changed for all the samples. It is seen from Fig. 6 that the maximum intensity of the basal plane texture of the as-annealed plate of 22.099 (see Fig. 1) is fiercely reduced to 12.76 and 7.83 for the central and outer regions, respectively. A much reduced intensity peak exists close to RD in these two regions. This may be resulted from the high density extension twins causing the inclination of the basal pole from ND about 87° towards RD [18]. Upon annealing, as

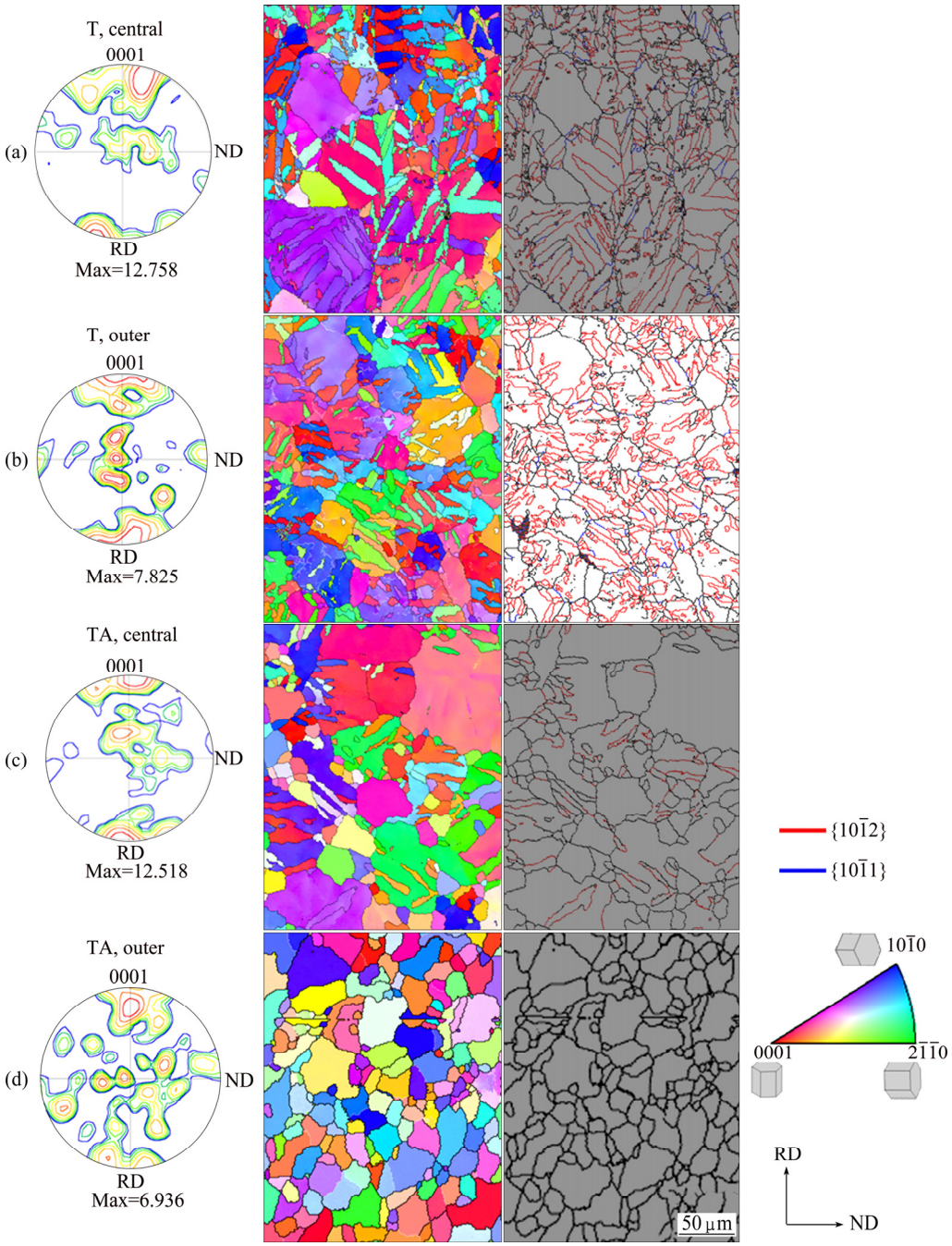

Fig. 6 (0001) pole figures, OIM maps and grain boundary maps in central and outer regions of samples after being prior-torqued (T) to γ=0.262 (a, b), and then followed by annealing (TA) (c, d) (In OIM maps and grain boundary maps, colors correspond to crystallographic orientation in the inverse pole figures. Black lines correspond to boundaries of misorientation $3°\leq\theta\leq15°$ and thick-black lines to $\theta>15°$. Red lines stand for the misorientation of 86° and thick-blue lines for 56°, which are boundaries for extension and contraction twins, respectively)

seen in Figs. 6(c) and (d), the intensity peaks of the center and outer regions stay nearly the same (from 12.758 to 12.518 for the center region, and from 7.825 to 6.936 for the outer region).

4 Discussion

4.1 Effect of torsion and subsequent annealing

When the as-annealed sample having a strong basal plane texture (Fig. 1) is compressed along the transverse direction of the plate, a tension strain is imposed on the *c*-axis of the grains under which circumstance the extension twins are readily activated [18]. As a result, it displays a flow curve with a yield plateau, which is a typical feature of {10$\bar{1}$2} extension twinning [19], as shown by broken curve in Fig. 2.

For the prior-torqued sample, it experiences a raise in the CD as well as UCS. XIN et al [19] reported a

similar phenomenon that such an increase in both CD and UCS can be resulted from grain refinement by $\{10\bar{1}2\}$ twinning caused by pre-straining. Such twins with rather broad width are recognized as $\{11\bar{2}0\}$ extension twins [18]. It is well known that $\{11\bar{2}0\}$ extension twinning in Mg alloys can easily take place under tensile load parallel to the *c*-axis or under compression load perpendicular to that, due to its low CRSS [18]. In torsion, the shear stress can be considered as a complex combination of extension and compression load perpendicular to the *c*-axis [12], so, it is reasonable to see so many extension twins in the torqued sample. High density dislocations and twin boundaries generated by prior-torsion of the Mg alloy can be a strong barrier to dislocation movement and twinning nucleation under subsequent compression, resulting in a clear strain-hardening performance [20] and an increase in YS and UCS, as seen in green lines of Fig. 2.

According to Eq. (1), the center region suffers much less shear strains compared with the outer one, but the volume fractions of tension twins of the outer and center regions show almost no difference, both are about 60%, as derived from the microstructure. This may be due to three reasons. Firstly, as a result of stress compatibility, the strain imposed on the center is far higher than that calculated from Eq. (1). Secondly, HONG et al [21] reported that $\{10\bar{1}2\}$ twins have completely nucleated at a small deformation (about 2%), grown between a strain of 2% and 6%, and then coalesced. With a strain of 8%, most grains are nearly completely twined. The strains that the center and the outer regions suffered have both already reached this degree of deformation. Thus, nearly no difference appears on volume fractions of these twins. Thirdly, except the occurrence of twins, there are also other types of deformation modes happening in these two areas, so there is no doubt that the volume of dislocation tangles in the outer region could be far more than that in the center because more strains occur in the outer region. Although this cannot be seen from the optical microstructure, it can be proved by the fact that the hardness in the outer region is much higher than that in the central area as shown in Fig. 5.

During annealing, different microstructures are developed for the center and outer regions on the cross section of the torqued sample. This suggests that static recrystallization (SRX) and recovery occurring in these two regions depend largely on the amount of prior shear strains, which can provide driving force needed for SRX. Larger prior shear strain imposing in the outer region leads to more dislocations and twins to assist its deformation and thus storing more deformation energy. More deformation energy means that nucleation sites can be more readily formed. It is concluded, therefore, that the occurrence of recovery and recrystallization in these two regions depends on the amount of shear strain applied, resulting in a gradient microstructure, i.e., refined grains with no twins in the outer region and coarser and recovered grains with some remaining twins in the central region. Such special microstructures developed during prior torsion and annealing are similar to a gradient microstructure developed by using bidirectional bending and static recrystallization by HUO et al [22].

4.2 Analysis for enhanced ductility and reduced asymmetry

It should be noted that a great increment in the ductility was achieved for the torqued sample followed by annealing. This may be ascribed to the grains being refined and the texture being weakened and randomized. The gradient microstructure derived from the torsion and annealing process may also help the ductility enhancement as reported by HUO et al [22].

KOIKE et al [23] have shown that the activation of non-basal slips is beneficial for the enhancement of the ductility of Mg alloys. The finer grain structure attained for the torqued sample followed by annealing means that it will have a higher volume fraction of grain boundaries. In order to deform the Mg alloy with finer grains to the same degree as the one with larger grains, more non-basal dislocation slips may be needed to maintain the compatibility and continuity.

According to the studies of CHINO et al [24] and HA et al [25], random or weaker texture will also be helpful to increase the ductility of magnesium alloy, as more slip systems are in the favorable directions with larger Schmid factors.

The tension–compression yield strength asymmetry in textured Mg alloys is closely related to the occurrence of $\{10\bar{1}2\}$ extension twins [7,26]. In our study of the tested as-annealed sample along TD direction of the as-annealed plate, when under compression, $\{10\bar{1}2\}$ twinning should dominate the deformation and the low critical resolved shear stress (CRSS) of the $\{10\bar{1}2\}$ twinning [7] results in quite low yield strength [27]. However, when under tension along transverse direction, the prismatic slip of $\langle a \rangle$ dislocation with high CRSS is suspected to control the macroscopic yield at room temperature [20]. Thus, large yield strength distinction appears during tension and the compression along transverse direction of the as-annealed plate. It is well reported that the texture and grain size of wrought Mg alloys are the two main factors that influence the occurrence of extension twinning. Therefore, the fiercely reduced yield strength asymmetry in our studied AZ21 Mg alloy should be related to the texture and grain size

developed during torsion and annealing process. During torsion, the rod suffered a great deal of shear strain, causing grains to rotate and form extension twins (Figs. 3(a) and (b)) which can refine the original grains. When under annealing, as seen from Figs. 3(c) and (d), the gradient microstructure was further refined. As extension twins are more reluctant to be activated in finer grains, the reduction of tension−compression yield strength asymmetry can be obtained to some extent [7]. In addition, when the texture becomes weakened and randomized, the occurrence of extension twins will also be greatly inhabited [6]. This should also help the reduction of tension−compression yield strength asymmetry.

It is concluded, therefore, that the development of the grains refinement, randomized and weakened texture as well as a gradient microstructure all contribute to such a dramatic increase in the compression ductility and the much lessened asymmetry.

5 Conclusions

1) The yield strength, ultimate compression strength and compression ductility of the as-annealed AZ21 Mg alloy plate can be raised simultaneously by prior-torsion. After subsequent annealing, the ductility increased further to the maximum value of more than twice that of the as-annealed one. The compression ductility of the torqued and subsequently annealed AZ21 Mg alloy increased with the increase in the prior shear strain.

2) Through torsion and subsequently annealing, a significant reduction was obtained for tension−compression yield asymmetry of the sample.

3) Dramatic increase in compression ductility and much reduced asymmetry of the material should result from the development of a gradient microstructure with refined grains, and also weakened and randomized texture.

Acknowledgements

The authors would gratefully acknowledge Dr. J. FOUSE from the State of Hawaii/DOH/EMD/CWB for numerous stimulating discussion.

References

[1] HIRSCHA J, Al-SAMMAN T. Superior light metals by texture engineering optimized aluminum and magnesium alloys for automotive applications [J]. Acta Materialia, 2013, 61(3): 818−843.

[2] LI Hui-zhong, WEI Xiao-yan, OUYANG Jie, JIANG Jun, LI Yi. Hot deformation behavior of extruded AZ80 magnesium alloy [J]. Transactions of Nonferrous Metals Society of China, 2013, 23(11): 3180−3185.

[3] YANG X Y, ZHU Y K, MIURA H, SAKAI T. Static recrystallization behavior of hot-deformed magnesium alloy AZ31 during isothermal annealing [J]. Transactions of Nonferrous Metals Society of China, 2010, 20(7): 1269−1274.

[4] GUO Fei, ZHANG Ding-fei, YANG Xu-sheng, JIANG Lu-yao, PAN Fu-sheng. Microstructure and texture evolution of AZ31 magnesium alloy during large strain hot rolling [J]. Transactions of Nonferrous Metals Society of China, 2015, 25(1): 14−21.

[5] YU Kun, RUI Shou-tai, WANG Xiao-yan, WANG Ri-chu, LI Wen-xian. Texture evolution of extruded AZ31 magnesium alloy sheets [J]. Transactions of Nonferrous Metals Society of China, 2009, 19(3): 511−516.

[6] YIN De-liang, WANG Jing-tao, LIU Jin-qiang, ZHAO Xiang. On tension–compression yield asymmetry in an extruded Mg−3Al−1Zn alloy [J]. Journal of Alloy and Compounds, 2009, 478(1−2): 789−795.

[7] XIN Yun-chang, ZHOU Xiao-jun, LIU Qin. Suppressing the tension–compression yield asymmetry of Mg alloy by hybrid extension twins structure [J]. Materials Science and Engineering A, 2013, 567: 9−13.

[8] HUANG Y, LANGDON T G. Advances in ultrafine-grained materials [J]. Materials Today, 2013, 16(3): 85−93.

[9] HUO Qing-huan, YANG Xu-yue, SUN Huan, LI Bin, QIN Jia, WANG Jun, MA Ji-jun. Enhancement of tensile ductility and stretch formability of AZ31 magnesium alloy sheet processed by cross-wavy bending [J]. Journal of Alloys and Compounds, 2013, 581: 230−235.

[10] HUO Qing-huan, YANG Xu-yue, MA Ji-jun, SUN Huan, QIN Jia, JIANG Yu-pei. Microstructural and textural evolution of AZ61 magnesium alloy sheet during bidirectional cyclic bending [J]. Materials Characterization, 2013, 79: 43−51.

[11] MA Ji-jun, YANG Xu-yue, HUO Qing-huan, SUN Huan, QIN Jia, WANG Jun. Mechanical properties and grain growth kinetics in magnesium alloy after accumulative compression bonding [J]. Materials and Design, 2013, 47: 505−509.

[12] ZHANG Hua, HUANG Guang-sheng, WANG Li-fei, ROVEN H J, XU Ze-bing, PAN Fu-sheng. Improved ductility of magnesium alloys by a simple shear process followed by annealing [J]. Scripta Materialia, 2013, 69(1): 49−52.

[13] KANG J Y, BACROIX B, BRENNER R. Evolution of microstructure and texture during planar simple shear of magnesium alloy [J]. Scripta Materialia, 2012, 66(9): 654−657.

[14] GUO X Q, WU W, WU P D, QIAO H, AN K, LIAW P K. On the Swift effect and twinning in a rolled magnesium alloy under free-end torsion [J]. Scripta Materialia, 2013, 69(4): 319−322.

[15] BEAUSIR B, TOTH L S, NEALE K W. Ideal orientations and persistence characteristics of hexagonal close packed crystals in simple shear [J]. Acta Materialia, 2007, 55(8): 2695−2705.

[16] BEAUSIR B, TOTH L S, QODS, F, NEALE K W. Texture and mechanical behavior of magnesium during free-end torsion [J]. Journal of Engineering Materials and Technology, 2009, 131(1): 011108-1.

[17] BISWAS S, BEAUSIR B, TOTH L S, SUWAS S. Evolution of texture and microstructure during hot torsion of a magnesium alloy [J]. Acta Materialia, 2013, 61(14): 5263−5277.

[18] BARNETT M R. Twinning and the ductility of magnesium alloys. Part I: “Tension” twins [J]. Materials Science and Engineering A, 2007, 464(1−2): 1−7.

[19] XIN Yun-chang, WANG Mao-yin, ZENG Zeng, NIE Ming-guang, LIU Qing. Strengthening and toughening of magnesium alloy by $\{10\bar{1}2\}$ extension twins [J]. Scripta Materialia, 2012, 66(1): 25−28.

[20] LOU X, LI M, BOGER R K, AGNEW S R, WAGONER R H. Hardening evolution of AZ31B Mg sheet [J]. International Journal of Plasticity, 2007, 23(1): 44−86.

[21] HONG S G, PARK S H, LEE C S. Role of $\{10\bar{1}2\}$ twinning characteristics in the deformation behavior of a polycrystalline magnesium alloy [J]. Acta Materialia, 2010, 58 (8): 5873−5885.

[22] HUO Qing-huan, YANG Xu-yue, MA Ji-jun, SUN Huan, WANG Jun, ZHANG Lei. Texture weakening of AZ31 magnesium alloy sheet obtained by a combination of bidirectional cyclic bending at low temperature and static recrystallization [J]. Journal of Materials Science, 2013, 48(2): 913−919.
[23] KOIKE J, KOBAYASHI T, MUKAI T, WATANABE H, SUZUKI M, MARUYAMA K, HIGASHI K. The activity of non-basal slip systems and dynamic recovery at room temperature in fine-grained AZ31B magnesium alloys [J]. Acta Materialia, 2003, 51: 2055−2065.
[24] CHINO Y, SASSA K, MABUCHI M. Enhancement of tensile ductility of magnesium alloy produced by torsion extrusion [J]. Scripta Materialia, 2008, 59: 399−402.
[25] HA S, KIM S J, HONG S, YIM C D, KIM D I, SUH J, OH K H, HAN H N. Improvement of ductility in magnesium alloy sheet using laser scanning treatment [J]. Materials Letters, 2010, 64: 425−427.
[26] LIU Ran, YIN De-liang, WANG Jing-tao. Elimination of yielding asymmetry in extruded AZ80 alloy by ageing [J]. Transactions of Nonferrous Metals Society of China, 2014, 24(4): 915−921.
[27] KOIKE J, OHYAMA R. Geometrical criterion for the activation of prismatic slip in AZ61 Mg alloy sheets deformed at room temperature [J]. Acta Materialia, 2005, 53(7): 1963−1972.

扭转及退火工艺对 Mg−2Al−1Zn 轧板塑性及拉压不对称性的改善

王 军[1,2]，杨续跃[1]，李 祎[1]，肖振宇[1]，张笃秀[1]，Taku SAKAI[3]

1. 中南大学 材料科学与工程学院 有色金属材料科学与工程教育部重点实验室，长沙 410083；
2. Institute for Frontier Materials, Deakin University, Geelong 3125, Australia;
3. The University of Electro-Communications, Tokyo 182-8585, Japan

摘 要：采用光学显微镜及电子背散射技术(EBSD)等手段研究扭转及后续退火工艺对热轧板 Mg−2Al−1Zn 镁合金塑性及拉压不对称性的改善。室温扭转后，样品的屈服强度、抗压强度以及压缩塑性都得到同步提高；随着扭转应变量的增加，样品的压缩塑性提高；并且在退火后，扭转试样的塑性得到大幅度提升，断裂时的最大真应变为 0.279，是原始轧制态的 2 倍。此外，扭转及扭转/退火后的样品拉压不对称性得到明显改善。分析表明，镁合金样品塑性的大幅度提高及拉压不对称性的改善主要是由于在扭转及后续退火过程中生成晶粒得到细化的梯度组织，以及原始强基面板织构的弱化和随机化。

关键词：镁合金；显微组织；扭转；不对称性；织构；孪晶

(Edited by Xiang-qun LI)